

## Temperature, density, and electric-field effects on electron mobility in nitrogen vapor

Toshinori Wada and Gordon R. Freeman

*Chemistry Department, University of Alberta, Edmonton, Canada T6G 2G2*

(Received 4 April 1980)

A detailed study of the effect of temperature on electron mobility in low-density nitrogen gas has revealed a Ramsauer-Townsend minimum in the scattering cross section at  $1.7 \times 10^{-16} \text{ cm}^2$  and  $15 \pm 2 \text{ meV}$ . The cross sections at  $\epsilon < 0.010 \text{ eV}$  are much larger than those previously reported. Energy gained by the electrons from the field is imparted to the molecules mainly through inelastic collisions, down to mean energies of a few meV. With increasing gas density the temperature coefficient  $\theta_{n,T} = (\partial \log(\mu n) / \partial \log T)_{n,T}$  near the vapor-liquid coexistence curve increases from  $-0.6$  at the low-density limit and  $80 \text{ K}$  to zero at  $n/n_c \geq 0.5$  and  $T/T_c > 0.97$ . While  $n/n_c$  increases from  $0.5$  to  $1.0$  along the coexistence curve, the density-normalized mobility  $\mu n$  decreases from  $14$  to  $1.0$  ( $10^{22}$  molecule/cm Vs) and the electric-field effect  $d\mu/dE$  changes sign from negative to positive. This behavior at high densities is attributed to electron capture,  $e^- + \text{N}_2 \rightleftharpoons \text{N}_2^- \rightleftharpoons \text{N}_2^-(\text{N}_2) \rightleftharpoons \text{N}_2^{2-}$  and so on. The capture coefficient  $\nu_c$  decreases with increasing electron energy.

### I. INTRODUCTION

When a new effect is discovered in gas-phase electron transport, attempts to understand it must involve studies in systems comprised of simple molecules. The monatomic molecule systems that have become standard are helium, argon, and xenon. The diatomic molecules most commonly used are hydrogen and nitrogen. In this context the behavior of low-energy electrons in gaseous nitrogen has been of periodic interest for nearly six decades.<sup>1-15</sup>

Studies of the effect of gas density on electron transport have uncovered a quasilocalized state of electrons in dense gases at temperatures near the gas-liquid coexistence region.<sup>16-23</sup> The state was discovered in systems comprised of nonpolar polyatomic molecules (hydrocarbons)<sup>16, 18</sup> and confirmed in the monatomic molecule system xenon.<sup>17</sup> We now extend the study to diatomic molecules, nitrogen.

The mobility of electrons in nitrogen gas has been reported to decrease by 2% as the density was increased from  $0.6$  to  $7$  ( $10^{19}$  molecule/cm<sup>3</sup>) at  $77.6 \text{ K}$  and  $0.03 \text{ Td}$ ,<sup>12</sup> and by 16% between  $3$  and  $97$  ( $10^{19}$  molecule/cm<sup>3</sup>) at  $293 \text{ K}$  and  $0.12 \text{ Td}$ .<sup>24</sup> Much larger effects are expected at higher densities and at lower temperatures and field strengths.

### II. EXPERIMENTAL

#### A. Material

Matheson Ultra High Purity nitrogen (99.9995%) was used. The gas was introduced into a vacuum system, which was initially evacuated to  $< 10^{-5}$  Pa ( $< 10^{-7}$  torr), under a pressure in excess of  $1$  atm through two cold traps at  $113 \text{ K}$ . The nitro-

gen was passed through a  $60 \text{ cm}$  column of copper grains at  $500 \text{ }^\circ\text{C}$ . The copper grains were pre-treated with hydrogen at  $500 \text{ }^\circ\text{C}$  until no further water was deposited on the surface of a cold trap. The column of copper grains was then evacuated to  $< 10^{-5}$  Pa for several days, keeping the temperature at  $500 \text{ }^\circ\text{C}$ . The treated nitrogen was then bubbled through a sodium-potassium alloy, transferred to a fresh potassium mirror, and condensed on it at  $77 \text{ K}$ . The liquid sample was maintained on the mirror overnight, then transferred to a fresh mirror. The mirror to mirror transfer was repeated several times. A fresh potassium mirror was generated under vacuum each time. Finally, a measured amount of liquid sample was transferred to a conductance cell and sealed under the gas pressure at solid nitrogen temperature.

#### B. Equipment

The conductance cell for most of the measurements was of the thick-glass-walled type which could contain a pressure of  $60 \text{ atm}$ .<sup>25</sup> The distance between the parallel electrodes was  $0.32 \text{ cm}$  and the effective area of the collecting electrode was  $2.5 \text{ cm}^2$ . Prior to filling with the sample, the cell was degassed by heating to  $250 \text{ }^\circ\text{C}$  while evacuating to  $< 10^{-5}$  Pa, then coated on the outside, except for the high-voltage side arm, with Aqua Dag for grounding.

For the lowest densities a "low-pressure cell" with a larger volume between the plates was used. The design was similar to that shown in Ref. 26, but the distance between the collector and high-voltage electrodes was  $1.00 \text{ cm}$ . The diameter of the collector was  $3.2 \text{ cm}$  and the space between the collector and guard was  $0.6 \text{ mm}$ . The distance between the plates was accurately measured with

a caliper and the effective area of the collector (8.3 cm<sup>2</sup>) was measured by way of the cell constant. The pressure of nitrogen in the cell at 77 K or 195 K was measured prior to sealing.

The high-pressure cell was placed in a thick-Styrofoam-walled cooling box which was similar to that described earlier.<sup>27</sup> The cell temperature was reduced by flowing cold nitrogen gas and measured with calibrated copper-constantan thermocouples. The temperature difference between the top and the bottom of the cell was <1 K and each temperature could be maintained at a constant value with a fluctuation of <0.5 K. The cell temperature was more accurately controlled in the experiments with the dense vapor near the critical region,  $T_{\text{top}} - T_{\text{bottom}} < 0.2$  K and  $\Delta T_{\text{top}} < 0.2$  K. The cooling box was placed in a well-grounded Faraday cage.

The low-pressure cell was cooled as above and heated in the manner described in Ref. 25(a).

The sample was irradiated with a 100 ns pulse of 1.7 MeV x rays, delivering  $1 \times 10^{10}$  eV/g to the gas. A dc voltage was applied to the high-voltage electrode by a Fluke (up to 6 KV) or Spellman (up to 30 KV) power supply through a series of well-grounded low pass filters. The RF filter is near the cell. An electron conductance transient (ECT) was observed using a preamplifier<sup>17</sup> and a Tektronix 7623 Oscilloscope. The 0–97% response time of the whole circuit was 40 ns. The ECT was measured with both positive and negative applied voltages.

### C. Determination of electron mobility

The electron mobility  $\mu$  and the electron drift velocity  $v_d$  were measured by a time-of-flight method. The determination of  $\mu$  has been described elsewhere<sup>21</sup> in detail and is mentioned here briefly. The mobility was determined using Eq. (1).

$$\mu = l^2/Vt_d, \quad (1)$$

where  $l$  is the distance between the electrodes,  $V$  is the applied voltage, and  $t_d$  is the time required for the electrons to drift the distance  $l$ . The ECT obtained at high-electric-field strengths was composed of three parts; the rising part, the linear decay part, and the tail part. The duration of the rising part was the same as the square radiation pulse width  $\tau$ . The drift time  $t_d$  was determined experimentally by  $[t_0 - (\tau/2)]$ , where  $t_0$  was the time when the extension of the linear decay crossed the base line ( $t = 0$  was taken at the starting point of the rising part).

For the ECT obtained at sufficiently low fields the effect of random diffusion of the electrons

during the drift to the collecting electrode was taken into consideration. In this case Eq. (2) was used to determine  $\mu$ <sup>21</sup>:

$$\begin{aligned} \mu &= v_d/E = l(l + \Delta x)/Vt_d \\ &= l^2 [1 + (2kT/eV)^{1/2}] / Vt_d, \end{aligned} \quad (2)$$

where  $\Delta x = (2Dt_d)^{1/2} = (2kT\mu l^2/e\mu V)^{1/2} = (2kT/eV)^{1/2}l$  is the mean distance of electron diffusion opposed to the field direction during the time  $t_d$ ,  $k$  is Boltzmann's constant,  $T$  is the absolute temperature, and  $e$  is the electron charge.

### D. Physical properties of the vapor

The densities  $n$  (molecule/cm<sup>3</sup>) of the saturated vapor were obtained as a function of temperature from Ref. 28. The critical temperature, pressure, and density of nitrogen are  $T_c = 126.2$  K,  $P_c = 33.5$  atm, and  $n_c = 6.7 \times 10^{21}$  molecule/cm<sup>3</sup>.<sup>29, 30</sup> The velocities of sound in the nitrogen gas were taken from Ref. 31.

## III. RESULTS

Electron mobilities were measured as functions of electric-field strength, temperature, and vapor density. The range of the density-normalized electric-field strength  $E/n$  was 0.001–5 Td (Td =  $10^{-17}$  V cm<sup>2</sup>/molecule). Measurements were made in the coexistence vapor from 77 K to  $T_c$ . The gas was also heated at several fixed densities from  $0.005 n_c$  to  $n_c$ .

### A. Electric-field effect

#### 1. Low density

The electron drift velocities  $v_d$  at  $n = 5.7 \times 10^{19}$  molecule/cm<sup>3</sup> and three different temperatures are plotted as functions of  $E/n$  in Fig. 1. At  $E/n$

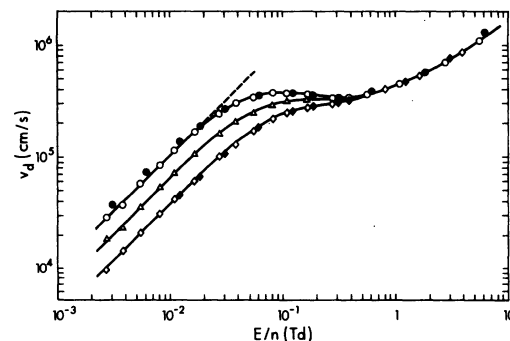


FIG. 1. Electron drift velocity  $v_d$  as a function of the density-normalized electric-field strength  $E/n$  at  $n = 5.7 \times 10^{19}$  molecule/cm<sup>3</sup>.  $\circ$ , 79 K;  $\triangle$ , 157 K;  $\diamond$ , 295 K. Reference 12,  $n \leq 6.6 \times 10^{19}$  molecule/cm<sup>3</sup>:  $\bullet$ , 77.6 K;  $\blacklozenge$ , 293 K. The dashed line has a slope of 1.0.

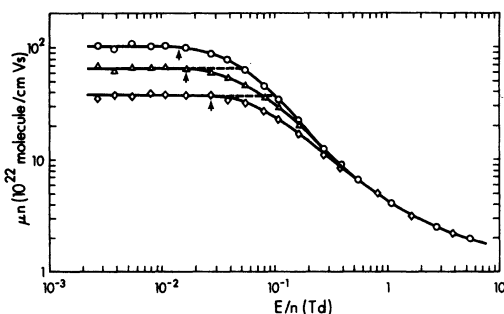


FIG. 2. Density-normalized electron mobility  $\mu n$  as a function of  $E/n$ . Symbols for temperature are the same as in Fig. 1. The arrows indicate  $(E/n)_{\text{thr}}$ , above which  $\mu n$  is dependent on  $E/n$ . The dashed lines are horizontal extensions of the electric-field-independent values of  $\mu n$  (used in Fig. 9).

$< 0.02$  Td  $v_d$  increases linearly with  $E/n$ , and at a fixed  $E/n$  its value decreases with increasing temperature. At  $E/n > 0.5$  Td, however,  $v_d$  is independent of temperature. At intermediate field strengths  $v_d$  is less sensitive to variation of  $E/n$  than it is at high and low fields. The present results are compared with those of Lowke<sup>12</sup> in Fig. 1.

To pick out the threshold field strength above which the electrons heat up it is preferable to plot the density-normalized electron mobility  $\mu n$  against  $E/n$ . In Fig. 2 one can readily see the low  $E/n$  region where  $\mu n$  is independent of  $E/n$  and the electrons are in thermal equilibrium with the molecules. The arrows indicate threshold values  $(E/n)_{\text{thr}}$  above which  $\mu n$  becomes field dependent. Above  $(E/n)_{\text{thr}}$   $\mu n$  decreases with in-

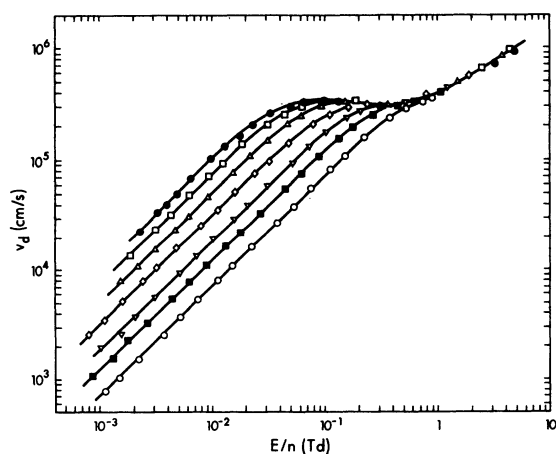


FIG. 3. Electron drift velocity in the coexistence vapor as a function of  $E/n$ . Densities and temperatures ( $10^{20}$  molecule/cm<sup>3</sup>, K):  $\bullet$ , 0.96, 77;  $\square$ , 5.0, 96;  $\triangle$ , 10, 106;  $\diamond$ , 19, 116;  $\nabla$ , 30, 122;  $\blacksquare$ , 35, 123;  $\circ$ , 42, 125.

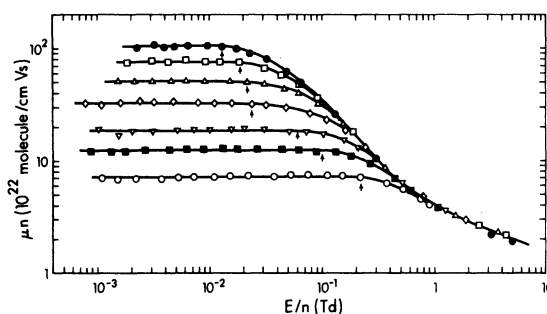


FIG. 4. Density-normalized electron mobility in the coexistence vapor as a function of  $E/n$ . Symbols for density and temperature are the same as in Fig. 3. The arrows indicate  $(E/n)_{\text{thr}}$ .

creasing field, which is the same tendency as when the temperature is increased at low  $E/n$ .

## 2. Along the coexistence curve

Figure 3 shows  $v_d$  as a function of  $E/n$  at seven densities of saturated vapor, from 0.96 to 42 ( $10^{20}$  molecule/cm<sup>3</sup>), with temperatures from 77 to 125 K. Increasing  $n$  results in a decrease of  $v_d$  at a fixed  $E/n$  in the low  $E/n$  region. At high  $E/n$  the  $v_d$  curves for different densities converge. The density effect was negligible at  $E/n > 0.5$  Td. Figure 4 shows the corresponding  $\mu n$  as a function of  $E/n$  and the  $(E/n)_{\text{thr}}$  values are marked. The value of  $(E/n)_{\text{thr}}$  increases from 0.013 Td at  $0.96 \times 10^{20}$  molecule/cm<sup>3</sup> to 0.22 Td at  $42 \times 10^{20}$  molecule/cm<sup>3</sup>. However, the corresponding threshold drift velocities  $v_d^{\text{thr}}$  are similar, being 1.3 and 1.6 km/s at the respective densities.

## 3. Near the critical region

Figure 5 shows the variation of  $\mu n$  against  $E/n$  in nitrogen near the critical region. The  $\mu n$  value for thermal electrons drops by an order of mag-

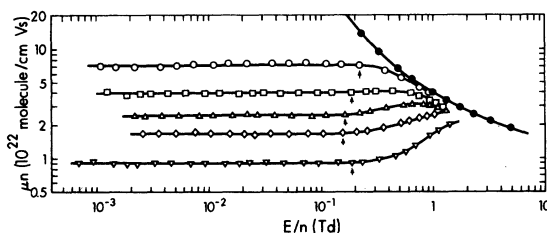


FIG. 5. Density-normalized electron mobility in nitrogen near the critical region as a function of  $E/n$ . Densities and temperatures ( $10^{20}$  molecule/cm<sup>3</sup>, K):  $\bullet$ , 0.96, 77;  $\circ$ , 42, 125.0;  $\square$ , 51, 126.3;  $\triangle$ , 59, 126.6;  $\diamond$ , 61, 127.2;  $\nabla$ , 67, 127.0 (used a conductance cell for liquid phase). The arrows indicate  $(E/n)_{\text{thr}}$ . See Fig. 6 and text for the determination of densities.

nitide when  $n$  increases by only 60%. As the density is increased above  $5.0 \times 10^{21}$  molecule/cm<sup>3</sup> the sign of the field dependence [ $d\mu n/d(E/n)$ ] at  $E/n > 0.2$  Td changes from negative to positive. The variation of  $\mu n$  seems to exhibit a peak. It appears that the value of  $E/n$  at which  $\mu n$  shows a maximum becomes bigger with increasing  $n$  and that after passing a maximum  $\mu n$  decreases to keep pace with the curve at the low density. The values of  $(E/n)_{\text{thr}}$  stay at 0.15–0.2 Td, except for the cusp that must occur at about  $4.8 \times 10^{21}$  molecule/cm<sup>3</sup> when the field dependence changes sign.

#### B. Gravity effect in the vapor near the critical region

A density gradient in fluids near the critical region is caused by the force of gravity, in cooperation with the rapid change of density with temperature and the large compressibility of the fluid.<sup>32</sup> The density of the vapor is smaller and that of the liquid is larger than the equilibrium value. This effect makes the decrease of  $\mu$  with  $T$  in the vapor less rapid than it would be if the vapor density were as large as it should be upon approaching the critical temperature from below (open circles in Fig. 6). The gravity effect was reduced in the liquid phase sample (filled circles in Fig. 6), by beginning at a supercritical temperature where the density gradient is small, and then reducing  $T$ . The dashed curve is regarded as the mobility variation in the vapor at the saturation density.

The vapor densities are considered to be the same when the mobilities are the same, because the mobility near the critical region is mainly

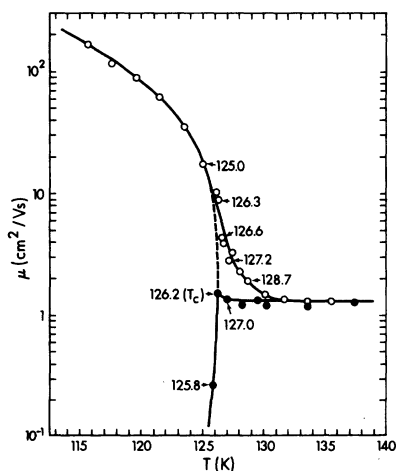


FIG. 6. Thermal electron mobility  $\mu$  in nitrogen near the critical point, as a function of temperature  $T$ .  $\circ$ , measurements done in a conductance cell designed for the gas phase;  $\bullet$ , measurements in a "liquid phase" cell. See text for the dashed curve.

determined by density rather than temperature. So, the open circles marked with temperatures in Fig. 6 are horizontally shifted to the dashed curve, then temperatures from the dashed curve give densities in saturated vapors.<sup>28</sup> The vapor densities so determined are used in Fig. 5 and the following sections.

#### C. Temperature effect

The mobility in the low-density gas was measured at temperatures from 77 to 585 K. The filled circles in Fig. 7 represent the average  $\mu n$  values from two fillings ( $n = 3.43 \times 10^{19}$  and  $4.86 \times 10^{19}$  molecule/cm<sup>3</sup>) of the "low-pressure cell." Mobilities from the two sets agreed within  $< 2\%$ . The difference between the results from the low- and high-pressure cells is partly due to the uncertainty in  $n$ . Values of  $\mu n$  reported earlier<sup>6,8,12</sup> are somewhat higher than the present ones at 77 K.

Figure 8 shows  $\mu n$  at several constant densities as a function of  $T$ , both axes being in log scale. The temperature coefficient of  $\mu n$  varies with density and temperature. In the lower density vapors the coefficient, taken as  $\theta_{\mu n, T} = (\partial \log(\mu n) / \partial \log T)_{n, T}$ , is negative and becomes more negative with increasing temperature; at the lowest density  $\theta_{100 \text{ K}} = -0.7$  and  $\theta_{250 \text{ K}} = -1.0$ . At the two lowest densities the temperature effect on  $\mu n$  is similar. With increasing density the coefficient becomes less negative. At densities  $n \geq 3.5 \times 10^{21}$  molecule/cm<sup>3</sup> the coefficient is nearly zero in the limited range of temperature measured above the coexistence curve. This seems also to hold in the

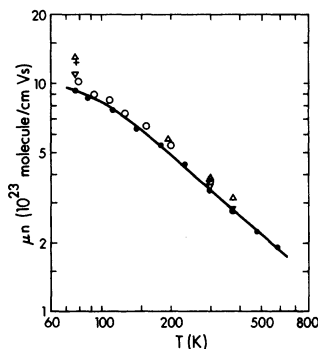


FIG. 7. Variation of  $\mu n$  with temperature in the low-density gas.  $\bullet$ , preferred values, "low-pressure cell" (LP), averages from two fillings with  $n = 3.43$  and  $4.86$  ( $10^{19}$  molecule/cm<sup>3</sup>).  $\circ$ , "high-pressure cell" (HP),  $n = 5.7 \times 10^{19}$  molecule/cm<sup>3</sup>.  $\nabla$ , Ref. 6;  $\triangle$ , Ref. 8,  $n \approx 3 \times 10^{19}$  molecule/cm<sup>3</sup>.  $+$ , Ref. 12, at lowest field strength measured, see Fig. 15. —, calculated from Eq. (5) and the cross sections in Fig. 11.

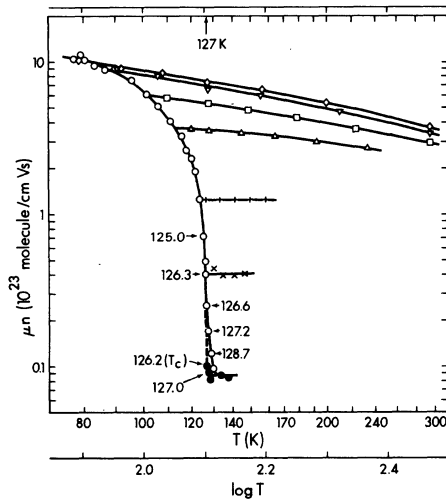


FIG. 8. Variation of the temperature dependence of  $\mu n$  with density.  $n$  ( $10^{20}$  molecule/cm<sup>3</sup>):  $\diamond$ , 0.57;  $\nabla$ , 2.0;  $\square$ , 8.0;  $\triangle$ , 18;  $+$ , 35;  $\times$ , 50;  $\bullet$ ,  $n_c = 67$ , "liquid cell";  $\circ$ , coexistence vapor. See Fig. 6 and text for explanation of the dashed curve and results near the critical region.

supercritical fluid ( $n_c = 6.7 \times 10^{21}$  molecule/cm<sup>3</sup>), as shown in Fig. 6.

#### IV. DISCUSSION

##### A. Low density gas

###### 1. Effect of electric field

The electron mobility decreases upon increasing either the electric-field strength above a threshold value or the temperature (Fig. 2). The mean electron energy increases under both circumstances, so when the electron interacts with only one molecule at a time the effects of electric field and temperature on  $\mu$  are expected to be similar. The characteristic energy of the electrons,  $\epsilon_\kappa = eD/\mu$ ,<sup>9</sup> is related to the Townsend energy factor  $\kappa$  by  $\epsilon_\kappa = \kappa kT$  for a Maxwellian distribution. The values of  $\kappa$  as a function of  $E/n$  at a given  $T$  are obtained from  $D/\mu$  data.<sup>10, 11, 14</sup> The approximation is made that the mean energies of the electrons are the same. The value of  $\mu n$  at 79 K and  $E/n = 0.10$  Td is the same as the field independent value at 295 K (Fig. 2), so the value of  $\kappa$  at 79 K and 0.10 Td is  $295/79 = 3.7$ . By using plots such as those in Fig. 2, drawing a horizontal extension of the field independent  $\mu n$  for a given  $T$  to intersect the curve for 79 K gives the value of  $E/n$  at which  $\kappa = T/79$  in the gas at 79 K. Values of  $T/79$  obtained in this way are plotted against  $E/n$  in Fig. 9. The values are similar to those of  $\kappa$  at 77 K obtained from  $D/\mu$  data of Warren and Parker<sup>10</sup> (Fig. 9).

The mean fractional energy loss  $\eta$  of a low-energy electron in a collision with a molecule is given

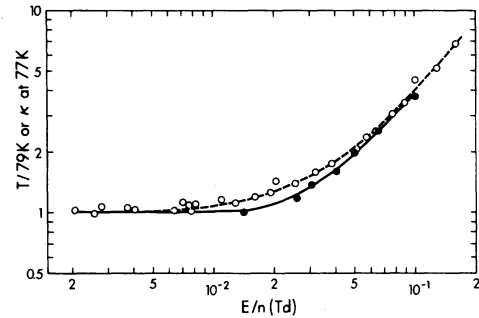


FIG. 9. Plot of  $T/79$  against  $E/n$  for electrons in low-density nitrogen at 79 K ( $\bullet$ , see text).  $n = 5.7 \times 10^{19}$  molecule/cm<sup>3</sup>.  $\circ$ , Townsend energy factor  $\kappa$  in low-density nitrogen at 77 K, obtained from  $D/\mu$  data in Ref. 10.

by<sup>33</sup>

$$\eta = F m v_d^2 / 3 \kappa k T, \quad (3)$$

where  $m$  is the electron mass, and the numerical factor  $F$  is  $3\pi/4$  when the electron velocity distribution is Maxwellian and the scattering cross section  $\sigma_v$  does not vary with the electron random velocity  $v$ . For an elastic collision the mean fractional energy loss  $\eta_e$  is given by<sup>33</sup>

$$\eta_e = S(m/M)(1 - \kappa^{-1}), \quad (4)$$

where  $M$  is the mass of the molecule and the numerical factor  $S$  is  $\frac{8}{3}$  for a Maxwellian distribution. The frequency of elastic collisions  $\nu_e$  exceeds greatly the frequency of inelastic collisions  $\nu_{in}$ ,<sup>9, 13</sup> so the quantity  $(\eta - \eta_e)/\eta_e$  represents the ratio of the energies lost in inelastic collisions to elastic collisions,  $\eta_{in} \nu_{in} / \eta_e \nu_e$ . In Fig. 10  $(\eta - \eta_e)/\eta_e$  is plotted as a function of  $\epsilon_\kappa$ , the electron energy having been increased by increasing  $E/n$  at 79 and 295 K, or by increasing temperature. The value of  $\kappa$  at each  $E/n$  was obtained from  $D/\mu$  data in Ref. 10 for 77 K, and Refs. 11 and 14 for 293 K. For the open circles in Fig. 10  $\eta$  and  $\eta_e$  were determined at  $(E/n)_{thr}$ , indicated by the arrows in Fig. 2, using  $\kappa$  at  $T$  estimated by  $(1 - 1.33/\sqrt{T})^{-1}$  which connects  $\kappa = 1.17$  at 77 K (Ref. 10) with  $\kappa = 1.09$  at 293 K.<sup>11, 14</sup> In the open circle systems the energy was changed thermally, so the energies of the molecules as well as that of the electrons changed.

The value of  $(\eta - \eta_e)/\eta_e$  increases with decreasing  $\epsilon_\kappa$ , from 5 at 0.4 eV to about 150 at 0.01 eV (Fig. 10). Inelastic scattering is the dominant process that moderates the electron energy. The electrons lose a large proportion of their energy in a small proportion of the total collisions. In this region rotational excitation of the molecules is the dominant energy loss process. (This indi-

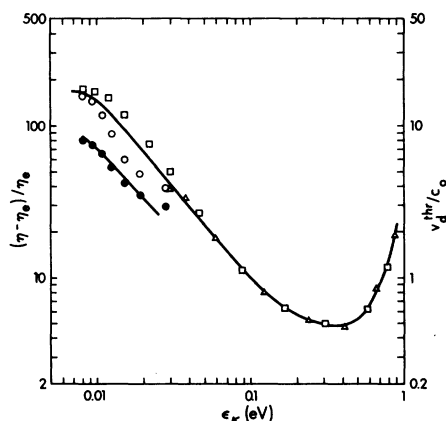


FIG. 10. Plots of ratios  $(\eta - \eta_e)/\eta_e$  ( $\square, \triangle$ ) and  $v_d^{\text{thr}}/c_0$  ( $\bullet$ ) against the characteristic energy of electrons  $\epsilon_k$  in low-density nitrogen,  $n = 5.7 \times 10^{19}$  molecule/cm<sup>3</sup>.  $\eta$  = mean fractional energy loss per collision;  $\eta_e$  = mean fractional energy loss per elastic collision;  $v_d^{\text{thr}}$  = threshold drift velocity above which  $v_d$  becomes nonlinear with  $E/n$ ;  $c_0$  = velocity of low-frequency sound. The electron energy was increased by increasing  $E/n$  at 79 K ( $\square$ ) and 295 ( $\triangle$ ), or by increasing temperature ( $\bullet, \bullet$ ).

cates that at thermal equilibrium the reversible exchange  $e^{-*} + \text{rot} \rightleftharpoons e^{-} + \text{rot}^*$  occurs with high probability where \* represents a quantum of energy.) The value of  $(\eta - \eta_e)/\eta_e$  passes through a minimum at  $\epsilon_k \approx 0.4$  eV and increases again with increasing  $\epsilon_k$ . The increase is attributed to direct vibrational excitation of the molecule, through a low-energy tail of the mechanism that involves the negative ion resonance states at 2.3 eV.<sup>34, 35</sup> The present result is in satisfactory agreement with Ref. 13, where it was reported that the fractional power input to vibrational excitation was greater than that to elastic plus rotational excitation processes at  $\epsilon_k > 0.3$  eV.

Elastic scattering of electrons by individual molecules is kinetically equivalent to scattering by phonons.<sup>36-38</sup> If elastic scattering were the dominant process that moderates the electron energy,  $v_d$  should become nonlinear with  $E/n$  when  $v_d \approx c_0$ , where  $c_0$  is the velocity of low-frequency sound in the medium.<sup>38</sup> The value of  $c_0$  in nitrogen at  $n = 5.7 \times 10^{19}$  molecule/cm<sup>3</sup> increases with temperature ( $c_0 = 20.3\sqrt{T}$  m/s), while the value of  $v_d^{\text{thr}}$  ( $= \mu n(E/n)_{\text{th}}$ , see Fig. 2) decreases. The ratio  $v_d^{\text{thr}}/c_0$  is also plotted in Fig. 10 as a function of  $\epsilon_k$ . The change of this ratio with energy is similar to that of  $(\eta - \eta_e)/\eta_e$ , although the magnitude of the former ratio is about 20 times smaller. The ratio  $v_d^{\text{thr}}/c_0$  is 8 at 79 K and 3 at 295 K, which implies that the electrons lose their energy mainly through inelastic processes under these condi-

tions. This supports the earlier conclusion<sup>23</sup> that the ratio  $v_d^{\text{thr}}/c_0$  is useful in assessing electron scattering processes.

## 2. Scattering cross sections

The temperature dependence of the thermal electron mobility in low-density nitrogen has been measured in much greater detail than previously (Fig. 7). This permits a more accurate determination of the scattering cross sections at low energies.

The method used to extract the cross sections from the mobilities was described earlier.<sup>9, 21</sup> Briefly, Eq. (5) was fitted to the experimental array of  $(\mu n, T)$  values represented by the filled circles in Fig. 7. The  $(\sigma_v, v)$  distribution was adjusted by trial and error until the fit was satisfactory:

$$\mu n = 5.23 \times 10^{-14} T^{-2.5} \times \int_0^{\infty} (v^3/\sigma_v) \exp(-3.30 \times 10^{-12} v^2/T) dv. \quad (5)$$

Equation (5) was integrated numerically, using 24 logarithmic steps between  $v = 2$  and  $37$  ( $10^4$  m/s), which was the sensitive range. The cross sections  $\sigma_v$  so obtained are shown in Fig. 11. The corresponding calculated values of  $\mu n$  are represented by the full line in Fig. 7.

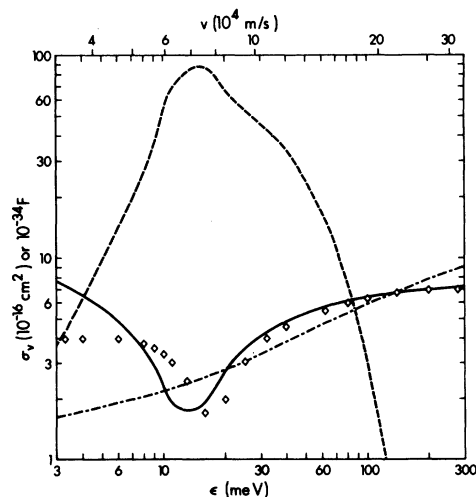


FIG. 11. Momentum transfer cross section  $\sigma_v$  as a function of electron energy  $\epsilon$  and velocity  $v$  in low-density nitrogen gas. —, present work;  $\diamond$ , estimated in an attempt to remove the minimum (see the Appendix); - · - · -, Ref. 13. ----,  $F = (v^3/\sigma_v) \exp(-3.30 \times 10^{-12} v^2/T)$ , at 200 K.  $F$  is inversely proportional to the probability of a scattering event, weighted for the velocity distribution at a given  $T$ .

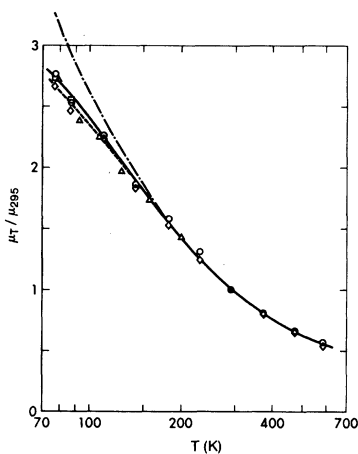


FIG. 12. Mobility ratio  $\mu_T/\mu_{295}$  as a function of temperature in nitrogen at the three lowest densities.  $n/10^{19}$  molecule/cm<sup>3</sup>:  $\circ$ , 3.43 (LP);  $\diamond$ , 3.43(LP), drift times estimated by computer processing of digitized conductance signals (see the Appendix);  $\square$ , 4.86 (LP);  $\triangle$ , 5.74 (HP). —, calculated from Eq. (5) and the full line cross sections in Fig. 11; ---, calculated with the  $\diamond$  cross sections in Fig. 11 (see Appendix); -·-, calculated with the cross sections from Ref. 13.

The data were checked for complications that might have been created by molecular clusters at the lowest temperatures. The ratio  $\mu_T/\mu_{295}$  was plotted against  $T$  for each of the three lowest densities (Fig. 12). If clusters had caused a detectable amount of quasilocalization at these densities, as the temperature was lowered the points for  $n=4.86$  and  $5.74$  ( $10^{19}$  molecule/cm<sup>3</sup>) would have become progressively lower than those for  $n=3.43 \times 10^{19}$  molecule/cm<sup>3</sup>. This was not observed, so it was concluded that quasilocalization was negligible in the lowest density gas.

There is a major difference between the present cross sections and those reported earlier<sup>9,13</sup> at  $\epsilon < 20$  meV. The main reason for the difference is that the earlier workers<sup>9,12</sup> reported the mobilities to be field dependent down to the lowest fields used (see the Appendix). The prolonged field dependences are not favored because they imply improbably low values of  $v_d^{\text{thr}}/c_0$  (Appendix). A minor difference was that the present cells were sealed, thereby fixing the value of  $n$  for a given temperature study. Earlier cells<sup>9,12</sup> were not sealed, but errors in  $n$  appear to have been small (Appendix).

At  $\epsilon > 100$  meV the cross sections reported by Phelps and co-workers are probably more reliable than ours (Fig. 7). The former were derived from  $D/\mu$  and  $v_d$  data.<sup>9,13</sup>

The shape of the cross-section curve at low energies (Fig. 11) may be attributed to the Ramsauer-Townsend effect. We do not wish to specu-

late further about it at this time. However, the Ramsauer-Townsend effect has recently been showing up in unexpected places.<sup>21,39</sup> The effect is defined phenomenologically and it requires a new theoretical attack.

## B. Effect of density

### 1. On the field effect

Increasing the gas density along the coexistence curve results in a decrease of  $\mu n$  for thermal electrons, a decrease in the field dependence of  $\mu n$ , and an increase of  $(E/n)_{\text{thr}}$  (see Fig. 4). The magnitudes of the changes in  $\mu n$  and  $(E/n)_{\text{thr}}$  with increasing  $n$  are shown in Fig. 13. There is a cusp in the variation of  $(E/n)_{\text{thr}}$  with  $n$ , associated with a change of sign of  $d\mu/dE$  at fields just above the threshold (Fig. 5). The change of sign of the field effect is due to electron localization in the dense gas.<sup>40</sup>

The threshold drift velocity is approximately constant on the low-density side of the cusp in the threshold field (Fig. 14). At  $n \leq 4.8 \times 10^{21}$  molecule/cm<sup>3</sup>,  $v_d^{\text{thr}} \approx 1.3$  km/s, which means that the energy lost by an electron in a collision is  $\Delta\epsilon \approx mv_d^2 \approx 1 \times 10^{-5}$  eV/collision [see Eq. (3)] in the threshold field. This quantity is apparently not affected by the localization processes that occur at densities up to  $4.8 \times 10^{21}$  molecule/cm<sup>3</sup>. Conversely, the localization processes are apparently little affected by field strengths up to the threshold in this density region. However, at higher densities localized states dominate the electron behavior, the field effect changes sign, and  $v_d^{\text{thr}}$  plunges (Fig. 14).

The speed of sound in saturated nitrogen vapor

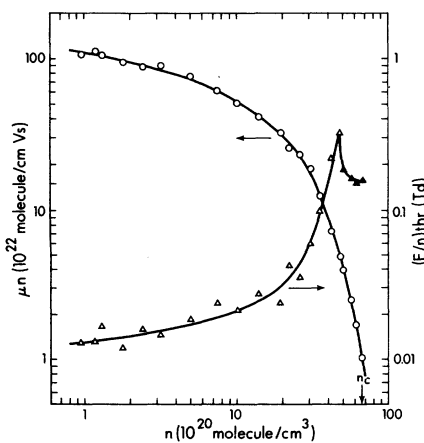


FIG. 13. Density dependences of  $\mu n$  for thermal electrons ( $\circ$ ), and  $(E/n)_{\text{thr}}$ , in the coexistence vapor.  $\triangle$ ,  $d\mu/dE$  is negative;  $\blacktriangle$ ,  $d\mu/dE$  is positive just above  $(E/n)_{\text{thr}}$ .

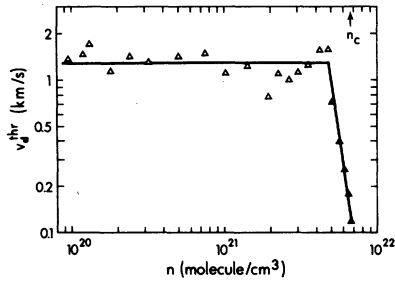
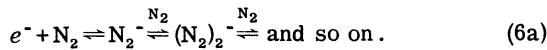


FIG. 14. Threshold drift velocity  $v_d^{\text{thr}}$  as a function of density. The symbols correspond to those in Fig. 13.

varies only slightly with density,  $173 \leq c_0(\text{m/s}) \leq 183$ .<sup>31</sup> Thus at  $n \leq 4.8 \times 10^{21}$  molecule/cm<sup>3</sup> the ratio  $v_d^{\text{thr}}/c_0 \approx 7.3$ . This means that for electrons near thermal energy in nitrogen vapor the electron energy is moderated mainly by inelastic collisions. It might also indicate that the ratio  $\eta_{in}\nu_{in}/\eta_e\nu_e$  is nearly independent of density in this range.

The increase of  $(E/n)_{\text{thr}}$  with density is due to the participation of an electron capturing process. One possibility for such a process is<sup>40</sup>



Several steps are included because the average lifetime of the ion increases rapidly at high densities.<sup>40</sup> The steps cannot yet be isolated, so one may write an average overall reaction



where  $\nu_a = \nu'_a n$  is the average attachment rate and  $\tau$  is the mean lifetime of the electron in the attached state;  $\tau$  increases with  $m$ , which increases with  $n$ . The collision frequency  $\phi$  of electrons, averaged over a long time, may be represented by

$$\phi = \nu(1 + \nu'_a n \tau)^{-1}, \quad (7)$$

where  $\nu$  is the average collision frequency of a quasifree electron with molecules.

The mobility of ions is several orders of magnitude smaller than that of electrons, so attachment decreases the measured drift velocity.<sup>41</sup> The average time that an electron remains in the quasifree state between trapping events is  $\nu_a^{-1} = (\nu'_a n)^{-1}$ . The time averaged mobility of the negative charge is

$$\mu = (\mu_0 \nu_a^{-1} + \mu_{\text{ion}} \tau) / (\nu_a^{-1} + \tau),$$

where  $\mu_0$  and  $\mu_{\text{ion}}$  are the mobilities of the unattached and attached electron, respectively. Since  $\mu_0 \gg \mu_{\text{ion}}$ , most of the drift of the negative charge

occurs when the electron is unattached, so one may neglect the drift of the ions. Thus,

$$\mu = \mu_0 \nu_a^{-1} / (\nu_a^{-1} + \tau) = \mu_0 (1 + \nu_a \tau)^{-1}.$$

In the present work the density-normalized mobility is mainly used, so we write

$$\mu n / (\mu n)_0 = (1 + \nu'_a n \tau)^{-1}, \quad (8)$$

where  $(\mu n)_0$  is the low-density value of  $\mu n$ . Equation (8) could also be obtained from Eq. (7), since the ratio  $\phi/\nu$  is equal to the fraction of time during which the electron is quasifree, and with the above approximations one obtains  $\mu n / (\mu n)_0 = \phi/\nu$ . The rapid decrease of  $\mu n$  at  $n > 2 \times 10^{21}$  molecule/cm<sup>3</sup> is attributed to an increasing value of  $m$  in Eq. (6) and a consequent increase of  $\tau$ .

At  $n > 0.7 n_c = 4.8 \times 10^{21}$  molecule/cm<sup>3</sup> the field dependence of  $\mu n$  is reversed and  $\mu n$  increases at  $E/n > 0.2$  Td (Fig. 5). The opposite type of field effect reversal, going from positive to negative values of  $d\mu/dE$ , has been observed in xenon,<sup>17</sup> methane,<sup>23</sup> neopentane,<sup>19,25a,32</sup> and ethane<sup>42</sup> at the respective reduced densities  $n/n_c = 2.0, 1.2, 1.3,$  and  $0.25$ . The first three occur in the liquid phase and are associated with large increases of  $\mu n$ , the maxima of which occur at higher densities. All four reversals are due to the lowering of the effective value of  $\sigma_v$  at low velocities, due to destructive interference of long-range attractive interactions.<sup>42</sup> The opposite behavior in nitrogen may be due to a decrease in the efficiency of temporary electron capture as the electron energy increases. Equation (8) shows that this would lead to an increase in  $\mu n$  with increasing  $E/n$ . Frommhold<sup>41</sup> has suggested that the capture process might involve rotational excitation, which would account for the enhanced values of  $\nu'_a$  for electron energies below 0.1 eV.

At still-higher field strengths  $d\mu/dE$  becomes negative again (Fig. 5), because the observed behavior is dominated by that of quasifree (uncaptured) electrons at high fields, which is described by Eq. (9)<sup>43</sup>:

$$(\mu n)_0 = \frac{-4\pi e}{3m} \int_0^\infty \frac{v^2}{\sigma_v} \frac{df_0}{dv} dv, \quad (9)$$

where  $f_0$  is the spherically symmetric term in the series expansion of the electron distribution function. Equation (5) results when a Maxwellian distribution is used for  $f_0$  in (9). At a field strength of 2 Td the characteristic energy is  $\epsilon_\kappa = 0.45$  eV,<sup>13</sup> in a range where the total scattering cross section is nearly independent of energy (Fig. 11 and Ref. 13), so  $\mu n$  decreases with increasing electron energy.

Thus the peak in a plot of  $\mu n$  against  $E/n$  for electrons in high-density nitrogen gas (Fig. 5) is



caused by the following changes with increasing  $v$  in the appropriate ranges of  $v$ : a decrease of  $v'_0$ ; a velocity dependence of the average scattering cross section which may be represented by a value of  $\alpha < 1$  in  $\sigma_{av} \propto v^{-\alpha}$ , at velocities where the effects of temporary electron capture have become sufficiently small.

## 2. On the temperature effect

The temperature coefficient of  $\mu n$  at low densities is negative. With increasing density the coefficient becomes less negative. At  $n \geq 0.5n_c = 3.5 \times 10^{21}$  molecule/cm<sup>3</sup> the coefficient is approximately zero in the limited range of temperature that could be measured above the coexistence curve (Fig. 8). This supports the suggestion that an electron localizes on a molecule, not in a cluster. The quasilocalization process that occurs in the high-density vapors of xenon<sup>17</sup> and a number of hydrocarbons<sup>16,18-21,23,42</sup> involves van der Waals clusters of molecules. It is very sensitive to temperature changes in a constant density vapor near the vapor-liquid coexistence region. The temperature coefficient  $\theta_{n,T} = (\partial \log(\mu n) / \partial \log T)_{n,T}$  in a constant density vapor near the coexistence curve increases rapidly with density. It has values in the vicinity of 15 near the critical region of a number of hydrocarbons<sup>21</sup> and xenon. For the quasilocalization process  $\theta_{n,T}$  is largest at temperatures just above the coexistence curve and diminishes rapidly with increasing temperature.<sup>21,22</sup> Electron quasilocalization evidently occurs at density fluctuations of adequate magnitude in the high-density vapors and decreases  $\mu n$  by a factor of at most 3 in the systems studied to date.

Although  $\theta_{n,T}$  in nitrogen increases from  $-0.6$  to zero with increasing density, the magnitude in the dense vapor is much too small to be attributed to quasilocalization. The large decrease in  $\mu n$  (by two orders of magnitude) and the small value of  $\theta_{n,T}$  are attributed to anion formation, process (6).

## APPENDIX

At fields  $\geq 25$  mTd the present values of  $\mu n$  in the low-density gas at 77 K agree with those of Pack and Phelps<sup>8</sup> and Lowke,<sup>12</sup> within the 3% uncertainty (Fig. 15). However, we found the mobilities to be independent of field strength below about 20 mTd, whereas the earlier workers reported continuing field dependence down to the lowest fields studied, which were 0.3 (Ref. 8) and 3 (Ref. 12) mTd (Fig. 15). The electron conductance signal is broadened by diffusion at low fields, which introduces an increasing subjective component into reading the drift time as the field

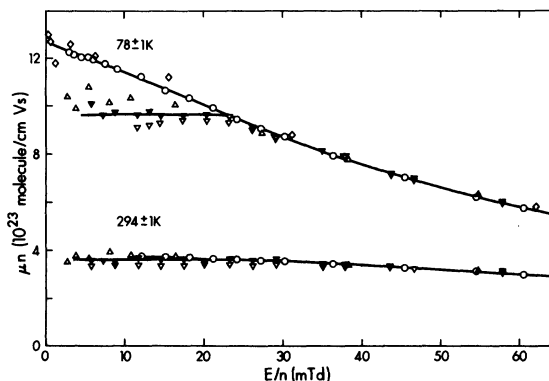


FIG. 15. Comparison of present data with that from Refs. 8 and 12 for the behavior of  $\mu n$  at low fields in the low-density gas.  $\diamond$ , Ref. 8, 77 K;  $\circ$ , Ref. 12, 78 and 293 K;  $\triangle$ , present, high pressure cell,  $n/10^{19} = 5.7$ , 79 and 295 K;  $\nabla$  and  $\triangledown$ , present, low pressure cell,  $n/10^{19} = 3.43$ , 77 and 295 K;  $\blacktriangledown$  determined from computer reading of time required for conductance signal to be reduced to 2% of the maximum.

strength is lowered. Our most recent data were recorded with a Tektronix model R7912 transient digitizer, with a 7A22 or 7A13 vertical plug-in, connected to a Texas Instruments 980A minicomputer and Zeta model 1200 digital plotter, instead of with the oscilloscope and camera. To check the visually read drift times and reduce the fluctuations due to subjectivity, we had the computer read the time required for the conductance signal to decrease to 2% of the maximum. This gave mobilities 2–6% larger than those obtained visually, but it confirmed the field independence below 20 mTd (Fig. 15).

Electrons in an electric field in nitrogen gas dissipate their energy mainly through inelastic collisions, even in the thermal energy range (Sec. IV A 1 and Fig. 10). Under these circumstances the value of the ratio of the threshold drift velocity to the speed of sound in the gas,  $v_d^{\text{thr}}/c_0$ , should be much greater than unity.<sup>22,23,42</sup> The low-field value of  $\mu n$  at 77 K reported by Pack and Phelps<sup>8</sup> was  $13.0 \times 10^{23}$  molecule/cm Vs, which would mean that the threshold field was  $\leq 0.3$  mTd (Fig. 15) and  $v_d^{\text{thr}}/c_0 \leq 0.2$ . This value put into Fig. 10 would be on or below the bottom axis at  $\epsilon_k = 0.0066$  eV and is much too low. Similarly, the data of Lowke<sup>12</sup> imply that  $v_d^{\text{thr}}/c_0 < 2.1$  at 77 K. While this limit is not theoretically impossible, Lowke did not observe a threshold field. His mobilities follow the same trend as those of Pack and Phelps and seem to be heading for a similar impossibly low value of  $v_d^{\text{thr}}/c_0$ . The present work indicates  $v_d^{\text{thr}}/c_0 = 10 \pm 2$  at 77 K.

At 293–295 K the difference between our data and Lowke's is smaller, but still significant.

TABLE I. Normalized mobilities of thermal electrons in low-density nitrogen.<sup>a</sup>

$T(K)$	$E/n$ (mTd)	$\mu n^b$ ( $10^{21}$ molecule/cm Vs)	$\mu_T/\mu_{295}$
76.7	6-23	$964 \pm 3^c$	2.67
86.5	6-23	$890 \pm 10$	2.47
111	6-18	$809 \pm 14$	2.24
140	5-26	$664 \pm 7$	1.84
181	6-21	$552 \pm 8$	1.53
231	5-26	$453 \pm 10$	1.25
295	6-29	$361 \pm 4^d$	1.00
373	6-46	$288 \pm 3$	0.80
473	17-47	$233 \pm 2$	0.65
587	9-58	$196 \pm 3$	0.54

<sup>a</sup>  $n = 3.43 \times 10^{19}$  molecule/cm<sup>3</sup>. Drift times read by computer and correction applied for diffusion (see text). The error introduced into  $(\mu_T/\mu_{295})$  by the 2% truncation method of measuring  $t_d$  should be small.

<sup>b</sup> Averages of values obtained from positive and negative applied voltages, to eliminate possible effects from contact and strain potentials.

<sup>c</sup> Average of two double sets measured three weeks apart on the same sample.

<sup>d</sup> Average of two double sets measured six days apart on the same sample.

Lowke reported field dependence down to the lowest field, 13 mTd, which implies  $v_d^{thr}/c_0 < 1.4$  (Fig. 15). Our work gives  $v_d^{thr}/c_0 = 3.5 \pm 0.5$  at 295 K.

Drift times at other temperatures were measured by computer in the above mentioned manner to test for field independent mobilities. The results and precisions are listed in Table I, along with the range of experimental fields over which  $\mu$  was deemed to be constant. The precisions of  $\mu n$  were 0.3-2%, averaged over 7-10 field strengths.

The values of  $\mu n$  and  $T$  in Table I were used to obtain scattering cross sections, with the aid of Eq. (5). The first trial set of cross sections was that of Englehardt, Phelps, and Risk.<sup>13</sup> Subsequent adjustments were made in such a way as to

try to avoid having a minimum in the cross section. When that failed we sought the flattest curve that would give an acceptable match to the experimental mobilities. The resulting cross sections are represented by the diamonds in Fig. 11 and the corresponding values of  $\mu_T/\mu_{295}$  are shown by the dashed line in Fig. 12.

The conclusion is that the electron scattering cross section of nitrogen has a minimum near  $1.7 \times 10^{-16}$  cm<sup>2</sup> and  $15 \pm 2$  meV.

#### ACKNOWLEDGMENT

This work was supported by the Natural Sciences and Engineering Research Council of Canada. We thank the staff of the Radiation Research Center for aid with the electronics.

<sup>1</sup>J. S. Townsend and V. A. Bailey, *Philos. Mag.* **42**, 873 (1921).

<sup>2</sup>C. Ramsauer and R. Kollath, *Ann. Phys. (Leipzig)* **4**, 91 (1930).

<sup>3</sup>R. A. Neilsen, *Phys. Rev.* **50**, 950 (1936).

<sup>4</sup>T. E. Bortner, G. S. Hurst, and W. G. Stone, *Rev. Sci. Instrum.* **28**, 103 (1957).

<sup>5</sup>L. G. H. Huxley, *J. Atmos. Terr. Phys.* **16**, 46 (1959).

<sup>6</sup>A. V. Phelps and J. L. Pack, *Phys. Rev. Lett.* **3**, 340 (1959).

<sup>7</sup>J. C. Bowe, *Phys. Rev.* **117**, 1411 (1960).

<sup>8</sup>J. L. Pack and A. V. Phelps, *Phys. Rev.* **121**, 798 (1961).

<sup>9</sup>L. S. Frost and A. V. Phelps, *Phys. Rev.* **127**, 1621 (1962).

<sup>10</sup>R. W. Warren and J. H. Parker, Jr., *Phys. Rev.* **128**, 2661 (1962).

<sup>11</sup>R. W. Crompton and M. T. Elford, *Proceedings of the Sixth International Conference on Ionization Phenomena in Gases*, Paris, 1963, Vol. 1, p. 337.

<sup>12</sup>J. J. Lowke, *Aust. J. Phys.* **16**, 115 (1963).

<sup>13</sup>A. G. Engelhardt, A. V. Phelps, and C. G. Risk, *Phys. Rev.* **135**, A1566 (1964).

<sup>14</sup>R. L. Jory, *Aust. J. Phys.* **18**, 237 (1965).

<sup>15</sup>J. Dutton, in *J. Phys. Chem. Ref. Data* **4**, 577 (1975).

<sup>16</sup>J.-P. Dodelet and G. R. Freeman, *J. Chem. Phys.* **65**, 3376 (1976).

<sup>17</sup>S. S.-S. Huang and G. R. Freeman, *J. Chem. Phys.* **68**, 1355 (1978).

<sup>18</sup>S. S.-S. Huang and G. R. Freeman, *Can. J. Chem.* **56**, 2388 (1978).

<sup>19</sup>T. György and G. R. Freeman, *J. Chem. Phys.* **70**, 4769 (1979).

<sup>20</sup>N. Gee and G. R. Freeman, *Chem. Phys. Lett.* **60**,

- 439 (1979).
- <sup>21</sup>T. Wada and G. R. Freeman, *Can. J. Chem.* **57**, 2716 (1979).
- <sup>22</sup>I. György and G. R. Freeman, *J. Electrostatics* **7**, 239 (1979).
- <sup>23</sup>N. Gee and G. R. Freeman, *Phys. Rev. A* **20**, 1152 (1979).
- <sup>24</sup>R. Grünberg (a) *Z. Phys.* **204**, 12 (1967); (b) *Z. Naturforsch.* **23a**, 1994 (1968).
- <sup>25</sup>(a) J.-P. Dodelet and G. R. Freeman, *Can. J. Chem.* **55**, 2264 (1977). (b) T. Wada and G. R. Freeman, *Phys. Rev. Lett.* **42**, 715 (1979).
- <sup>26</sup>J.-P. Dodelet, K. Shinsaka, U. Kortsch, and G. R. Freeman, *J. Chem. Phys.* **59**, 2376 (1973).
- <sup>27</sup>J.-P. Dodelet and G. R. Freeman, *Can. J. Chem.* **55**, 2893 (1977).
- <sup>28</sup>T. R. Strobridge, *Natl. Bur. Stand. Tech. Note* 129A (U.S. GPO, Washington, D. C., 1963).
- <sup>29</sup>R. R. Dreisbach, *Adv. Chem. Ser.* **22** (1959).
- <sup>30</sup>R. C. Reid, J. M. Prausnitz and T. K. Sherwood, *The Properties of Gases and Liquids* (McGraw-Hill, New York, 1977).
- <sup>31</sup>R. T. Jacobsen and R. B. Stewart, *J. Phys. Chem. Ref. Data* **2**, 757 (1973).
- <sup>32</sup>S. S.-S. Huang and G. R. Freeman, *J. Chem. Phys.* **69**, 1585 (1978).
- <sup>33</sup>L. G. H. Huxley and R. W. Crompton, *Atomic and Molecular Processes*, edited by D. R. Bates (Academic, New York, 1962), p. 335, see pp. 351-353.
- <sup>34</sup>R. Haas, *Z. Phys.* **148**, 177 (1957).
- <sup>35</sup>G. J. Schulz, *Phys. Rev.* **116**, 1141 (1959).
- <sup>36</sup>F. B. Pidduck, *Proc. London Math. Soc.* **15**, 89 (1916).
- <sup>37</sup>W. Shockley, *Bell Syst. Tech. J.* **30**, 990 (1951), see pp. 1018-1024.
- <sup>38</sup>M. H. Cohen and J. Lekner, *Phys. Rev.* **158**, 305 (1967), and references therein.
- <sup>39</sup>G. R. Freeman, I. György, and S. S.-S. Huang, *Can. J. Chem.* **57**, 2626 (1979).
- <sup>40</sup>T. Wada and G. R. Freeman, *J. Chem. Phys.* **72**, 6726 (1980).
- <sup>41</sup>L. Frommhold, *Phys. Rev.* **172**, 118 (1968).
- <sup>42</sup>N. Gee and G. R. Freeman, *Phys. Rev. A* **22**, 301 (1980).
- <sup>43</sup>L. G. H. Huxley and R. W. Crompton, *The Diffusion and Drift of Electrons in Gases* (Wiley, New York, 1974), Chapters 3 and 13, pp. 69-70, 526-584.